Al Furat Journal of Innovations in Engineering Applications (AJIEA)
ISSN - 3105-3149

NUMERICAL SIMULATION OF DOUBLE PIPE HEAT EXCHANGER BY USING WATER_ZNO NONO FLUID

Hajir Hayder[1], Rana Ali Hussein[1], Ali A. Abbas Aljanabi[1*]

[1]Department Mechanical Power Engineering, Mussaib Technical College, Al Furat Al Awsat Technical University, 51006, Babil, Iraq
[*]Corresponding author E-mail: hajir.hayder.tcm14@student.atu.edu.iq

https://doi.org/10.46649/ajiea.v1.2.7a.30.12.2025

Abstract *A double-pipe heat exchanger was fabricated to experimentally investigate the thermal conductivity of distilled water with nanoparticle additives. Nanoparticles (0.05%) were dispersed in pure water to form a nanofluid. The system was tested at two flow rates: 4 and 6 L/min. Temperature and flow fields were studied during the simulations. A numeri-cal study was also carried out to further calculate the overall heat transfer coefficients and heat transfer rates for pure water and nanofluid nanoparticles with 0.05% mass fraction. Thermal performance was significantly increased with the application of the nanofluid, by these results. The overall heat transfer coefficient was higher than pure water by ~25% and ~35% for a flow rate of 4L/min and 6 L/min, respectively. Besides, bold heat transfer with good flow dynamics was shown for thenanofluid. Of the flow rates tested, 6 L/min resulted in a 10% increase in thermal performance when compared to the 4 L/min case, highlighting benefit of employing higher fluid flows for nanofluids within thermal systems. Results underscore the potential use of nanoparticles in improving heat exchanger efficiency and minimizing thermal energy losses, resulting in approximately 30% higher thermal efficiency than pure water for the same environmental and operational conditions*

.

Keywords: *Double pipe heat exchanger, Nano fluid, Thermal efficiency, Flow rate*

1. INTRODUCTION

Heat exchangers are extensively used in many industries [1]. Some of these methods to enhance heat transfer will probably decrease the need for a perfect container, involving pressure loss and heat transfer. As a result, the procedures should be chosen carefully. In addition, the realization of an acceptable high heat transfer rate in many technical applications, such as automotive engines, electric power systems, computers etc., is believed to be inevitable requirement [2]. Zinc oxide (ZnO) is a nanomaterial with good electrical and high thermal conductive properties, that makes this a strong competitor for enhancing Heat transfer in devices like heat exchanger [3]. Nanoparticle volume fraction higher leads ZnO- nanofluide to higher viscosity. On the other hand, the case of temperature dependent thermal conductivity was only motivated by clustering and aggregation of nanoparticles [4]. The investigation showed that the ZnO-water nanofluid possesses a count of relative viscosity on temperature in 35-55°C range and more ultrasonication originate aggregates with less fractal dimension. [5]. With the increase of nanoparticle concentration and crystallite size, a nanofluid base on ZnO in better thermal conductive along with low thermal resistance and disturbed temperature distribution were found [6]. Using a ZnO nanofluid with the

ATU- AJIEA, Volume:1, Issue: 2, 12, 30, 2025, © 2025 AJIEA, All Rights Reserved

shape factor > 3 should give similar performance to the water in terms of PEC along with little increase in Nusselt numbers compared to base fluid [7]. As we known, the thermal conductivity, density, and viscosity dispersed of the ZnO nanofluid were also nonlinearly affected by not only temperature and concentration but also particle size._particle size was observed to be greater than that of viscosity [8]. The addition of a ZnO nanofluid dispersed in xanthan gum has been shown to increase thermal and electrical conductivities up to 25% with increasing nanoparticle loading [9]. Results showed that the heat transfer over the base fluid increased by 12% In horizontal double-pipe counter-flow kind of heat exchanger with nanofluid of aluminum oxide and water [10]. A maximum cooling capacity improvement of 29% without degrading the electrical performance was achieved with a 0.5% ZnO nanofluid in PEMFC cooling system. [11]. It was found that is to explore a ZnO-water nanofluid in natural convection within a closed rectangular enclosure, examining the impacts of different factors such as heated wall location and nanoparticle volume concentration [12] The investigation uncovered that the zinc oxide nanofluid boosted recovery efficiency by 50% without electromagnetic (EM) energy, and that adding EM energy raised recovery performance by 23.3% through the ZnO nanoparticles' electrorheological influence [13]. Several studies were also conducted in the double pipe heat exchanger utilizing nanomaterials. Mango bark nanofluids' convective heat flow coefficient was assumed in a twin pipe heat exchanger experiencing turbulent circumstances. According to performance studies, the Nusselt number enhancement factor was 68% at Reynolds number (Re) = 5000 and 45% at Re = 13000, compared to the base fluid, the coefficient of heat transfer was twice as high. Heat transfer rates increased in some locations, which might be used to construct heat exchangers [14]. A studied on the impact of silver nanoparticles applied on heat exchangers as a coating material utilizing copper pipes discovered that the heat transfer coefficient and mass flow rate were improved by 95% when compared to plain copper pipes. This phenomenon was seen in countercurrent flow, which provides greater thermal transfer than co-current flow [15]. The experiment demonstrated that when a ZnO–water nanofluid is used in a counter-flow double-tube heat exchanger, the maximum performance ratio of 54% was achieved at 2 L/min volumetric flow rate and with 1% mass concentration of nanoparticle [16]. The double-pipe heat exchanger employing zinc oxide (ZnO) nanoparticle and alkaline water enhances the heat transfer rate, and thermal efficiency increases with the increase in nanoparticle concentration [17]. The researchers observed that application of ZnO-H2O nanofluid at a volume fraction of 0.06% with Reynolds number equal to 5500, enhance the Nusselt's number collector by 35%, and a thermal efficiency factor of 1.15 [18]. An investigation on a counter flow double-tube heat exchanger using ZnO- water nanofluids (30 nm, 0.5 -1 wt%) was reported by Bang et al. The nanofluid (20 °C) entered at 2-6 L/min into the annulus and passed through an inner tube, from which the hot water (65 °C, 4 L/min) evaporated. It was found that nanofluids were more effective than pure water, with a maximum effectiveness of 40% for 0.5 wt%. % and 54% at 1 wt. % using a flow rate of 2 L/min [19].

The performance of a two-pipe heat exchanger with thenanofluids of 0.05 w.t% ZnO is studied in this work. This paper examines the effect of ZnO nanofluids on filling performance andheat transfer capability, focusing on such critical parameters as heat productivity and heat transfercoefficient. Effect of different concentrations of ZnO nanoparticles on the overall performance of the heat exchanger is discussed for enhancing thermal effectiveness and maximum energy efficiency.

ATU- AJIEA, Volume:1, Issue: 2, 12, 30, 2025, © 2025 AJIEA, All Rights Reserved

Al Furat Journal of Innovations in Engineering Applications (AJIEA)
ISSN - 3105-3149

2. GOVERNING EQUATIONS

2.1. CONTINUITY EQUATION

- General Form (for compressible flow) [20]:

$$\frac{\partial \rho}{\partial t} + \nabla.(\rho\vec{v}) = 0 \qquad (1)$$

- For incompressible flow:

$$\nabla.\vec{v} = 0 \qquad (2)$$

- For steady, incompressible flow in a pipe:

$$a_1 v_1 = a_2 v_2 \qquad (3)$$

2.2. MOMENTUM EQUATION (NAVIER-STOKES EQUATION)

Momentum equations are inferred from Newton's second law, which includes pressure forces, viscous forces, and external forces acting on the flow. The momentum equation for a Newtonian fluid is expressed below in vector form [20]:

$$\frac{\partial}{\partial t}(\rho\vec{v}) + \nabla\cdot(\rho\vec{v}\vec{v}) = -\nabla p + \nabla\cdot\tau + \rho\vec{g}, \qquad (4)$$

where

- p pressure in pascal
- τ viscous stress tensor (Pa) that is directly proportional to the product of the viscosity of a fluid and its velocity gradients.
- $\vec{g}$ vector for gravitational body force $(\mathrm{m/s^2})$.
- the momentum equation in the $\mathrm{s, f}\ and\ \mathrm{n}$ −direction (component form) respectively is:

$$\frac{\partial}{\partial t}(\rho c) + \frac{\partial}{\partial s}(\rho c^2) + \frac{\partial}{\partial f}(\rho c i) + \frac{\partial}{\partial n}(\rho c w) = -\frac{\partial p}{\partial s} + \mu\left(\frac{\partial^2 c}{\partial s^2} + \frac{\partial^2 c}{\partial f^2} + \frac{\partial^2 c}{\partial n^2}\right)$$

$$\frac{\partial}{\partial t}(\rho i) + \frac{\partial}{\partial s}(\rho c i) + \frac{\partial}{\partial f}(\rho i^2) + \frac{\partial}{\partial n}(\rho i w) = -\frac{\partial p}{\partial f} + \mu\left(\frac{\partial^2 i}{\partial s^2} + \frac{\partial^2 i}{\partial f^2} + \frac{\partial^2 i}{\partial n^2}\right) \qquad (5)$$

$$\frac{\partial}{\partial t}(\rho w) + \frac{\partial}{\partial s}(\rho c w) + \frac{\partial}{\partial f}(\rho i w) + \frac{\partial}{\partial n}(\rho w^2) = -\frac{\partial p}{\partial n} + \mu\left(\frac{\partial^2 w}{\partial s^2} + \frac{\partial^2 w}{\partial f^2} + \frac{\partial^2 w}{\partial n^2}\right),$$

Where μ denotes the fluid's dynamic viscosity. c , i,w denote the components of the velocity in the s,f,n directions, respectively.

ATU- AJIEA, Volume:1, Issue: 2, 12, 30, 2025, © 2025 AJIEA, All Rights Reserved

2.3. ENERGY EQUATION (CONSERVATION OF ENERGY)

The equation of energy for fluid dynamics governs the conservation of energy, taking into consideration convection, heat conduction, and heat generated by viscous dissipation. The general form of the energy equation is [20]:

$$\frac{\partial}{\partial t}(\rho e) + \nabla \cdot \left(\vec{v}(\rho E + P)\right) = \nabla \cdot (K\nabla T) + \Phi, \qquad (6)$$

where

- e denotes the total energy per unit mass (J/kg), given by:

$$e = H - \frac{P}{\rho} + \frac{v2}{2} \qquad (7)$$

- Kthermal conductivity $(W/m \cdot K)$.
- H specific enthalpy (J/kg).
- T temperature (K).
- Φ viscous dissipation function, this measures the rate at which energy is dissipated through viscous forces.

The energy equation is critical in numerical modeling of heat transfer, for instance in conjugate heat transfer or applications in thermal control systems.

2.4. TURBULENCE MODEL

A number of turbulence models are available in ANSYS Fluent, each one based on how turbulence influences fluid flow. These models are constructed using additional transport equations that exhibit a natural turbulence characteristic [21].

$k{-}\varepsilon$ Model: In this two-equation model, the turbulence kinetic energy (k) and its dissipation rate (ϵ) are approximated by two extra transport equations.

$$\frac{\partial(\rho K)}{\partial T} + \nabla \cdot (\rho K \vec{v}) = \nabla \cdot (\frac{\mu_t}{\sigma_k}\nabla K) + G_l - \rho\epsilon \qquad (8)$$

$$\frac{\partial(\rho\epsilon)}{\partial T} + \nabla \cdot (\rho\epsilon \vec{v}) = \nabla \cdot (\frac{\mu_t}{\sigma_\epsilon}\nabla\epsilon) + C_1\frac{\epsilon}{k}G_k - C_2\rho\frac{\epsilon^2}{k}$$

In equation above $(C\varepsilon_1$ and $C\varepsilon_2)$ are constants. (G) is the generation term, $(\sigma k$ and $\sigma\varepsilon)$ denote the turbulent Prandtl numbers for (k) and (ε) respectively. (μt) denotes the turbulent (or eddy) viscosity. A combination of (k) and (ε) is employed to calculate the turbulent viscosity (μt):

ATU- AJIEA, Volume:1, Issue: 2, 12, 30, 2025, © 2025 AJIEA, All Rights Reserved

$$\mu_t = \rho C_\mu \frac{K^2}{\varepsilon} \qquad (9)$$

To simulate turbulent flow, was use the realizable k-ε turbulence model. The equations of modeled transport for k and ε in the realizable $K-\varepsilon$ model were as follows: Manual, user. "ANSYS FLUENT 22.0" Theory guide [20].

$$\frac{\partial}{\partial t}(\rho K) + \frac{\partial}{\partial S_j}(\rho k u_j) = \frac{\partial}{\partial S_j}\left[\left(\mu + \frac{\mu_t}{\sigma_k}\right)\frac{\partial K}{\partial S_j}\right] + G_l + G_n - \rho\varepsilon - Y_r + S_h \qquad (10)$$

and

$$\frac{\partial}{\partial t}(\rho\varepsilon) + \frac{\partial}{\partial S_j}(\rho\varepsilon u_j) = \frac{\partial}{\partial S}\left[\left(\mu + \frac{\mu_t}{\sigma_\varepsilon}\right)\frac{\partial \varepsilon}{\partial S_j}\right] + \rho C_1 S\varepsilon - \rho C_2 \frac{\varepsilon^2}{k + \sqrt{v\varepsilon}} + C_{1\varepsilon}\frac{\varepsilon}{k} C_{3\varepsilon} G_n + S_\varepsilon \qquad (11)$$

where

$$C_1 = \max\left[0.43, \frac{\eta}{\eta + 5}\right], \quad \eta = S\frac{k}{\varepsilon}, \quad S = \sqrt{2S_{IJ}S_{IJ}} \qquad (12)$$

2.5 HEAT TRANSFER RATE

Heat transfer rate through inner side (water or nanofluid) is:

$$Q_h = m_h cp_h^{\cdot}(T_{ho} - T_{hi}) \qquad (13)$$

The air temperature is subtracted from the water temperature to determine the amount of heat dissipation. This zone allows for reliable parameter measurement [22].

2.6 INNER SIDE HEAT TRANSFER COEFFICIENT (HI)

When working with nanofluids or water, Newton's equation of cooling serves to determine the coefficient of heat transfer on the inner side:

$$H = \frac{Q}{A.\Delta T} \qquad (13)$$

$$Q_h = h_i A_i \left(T_{m_{T_s}}\right), \qquad (14)$$

Where

$$T_m = \frac{T_{hi} + T_{ho}}{2} \qquad (16)$$

$$T_s = \frac{T_1 + \cdots + T_7}{7} \qquad (17)$$

ATU- AJIEA, Volume:1, Issue: 2, 12, 30, 2025, © 2025 AJIEA, All Rights Reserved

2.7. EFFECTIVENESS

Denotes the ratio of actual transmission of the heat to maximal transfer of the heat [23].

$$\varepsilon = \frac{Q_{actual}}{Q_{max}} \quad (18)$$

$$\varepsilon = \frac{m_h \dot{cp_h}(T_{out_}T_{in})}{m_{min}\dot{cp_{min}}(T_{h,in_}T_{c,in})} \quad (19)$$

$$\varepsilon = \frac{1 - exp\,[-NTU(1 - Cr)]}{1 - Cr\,exp\,[-NTU(1 - Cr)]}, \quad (20)$$

where

- $$Cr = \frac{C_{min}}{C_{max}} \quad (21)$$
- $C_{\ min}$: The smaller heat capacity rate between the two fluids ($C = \dot{m}.C_P$)
- $C_{\ max}$: The begger heat capacity rate between the two fluids ($C = \dot{m}.C_P$)

2.7. EFFECTIVENESS-NTU METHOD

The NTU Method is extremely useful for assessing heat exchangers with uncertain beginning temperatures. It creates a link between the heat exchanger's efficacy (ε) and number of transfer units.

2.8. NUMBER OF TRANSFER UNITS (NTU):

$$\mathrm{NTU} = \frac{\mathrm{UA}}{\mathrm{C_{min}}} = \frac{\mathrm{Q}}{\Delta \mathrm{T_{LM}} \mathrm{C_{min}}} \quad (22)$$

where $C_h = \dot{m}_h \dot{C}_{P_h}, C_c = \dot{m}_c \dot{C}_{P_c}$
C_{min}: The minimum value of $C_h$and C_C
C_{P_h}, C_{P_C}: Hot and cold fluids' specific heat capacities, respectively.

2.9 Nusselt Number

To assess the convective heat transfer performance of the nanofluid inside the inner tube, the Nusselt number was determined for all instances. The standard definition was used to get the local Nusselt number [23].

$$Nu = \frac{h\,D_h}{k} \quad (23)$$

where h is the convective heat transfer coefficient, $D_h$is the hydraulic diameter, and kkk is the thermal conductivity of the fluid. Furthermore, the average Nusselt number values were compared with the classical Dittus-Boelter correlation:

ATU- AJIEA, Volume:1, Issue: 2, 12, 30, 2025, © 2025 AJIEA, All Rights Reserved

$$\mathrm{Nu} = 0.023 Re^{0.8} Pr^{n} \quad (24)$$

Using n=0.4 for heating conditions. The agreement was reasonable, verifying the numerical results. Also, the use of ZnO-water nanofluid led to a substantial enhancement of Nusselt compared with that for pure water, reflecting better convective heat transfer. The enhanced performance is attributed to the increased thermal conductivity and energy transfer by dispersion of the nanoparticles. The results provide the evidence that nanofluids are able to enhance the heat exchanger performance in industrial applications..

3. NANOFLUID THERMO-PHYSICAL PROPERTIES

3.1. DENSITY

The mass-to-volume ratio is the measure of a substance's density. The classical mixing law is a commonly used equation for estimating density. According to traditional mixing principle, The nanofluid's density It can be stated as [23]:

$$\rho_{nf} = \rho_{np}\emptyset + (1-\emptyset)\rho_{bf}\ , \quad (25)$$

where ρ_{nf} denotes the nanofluid's effective density, ρ_{bf} denotes the water base fluid's density, $\emptyset$ denotes the nanoparticles volume fraction, and ρ_{np} denotes the density of the nanoparticles (ZnO) [20].

3.2. SPECIFIC HEAT

The nanofluids' specific heat may be described as an expression of volume concentration and density using mixing law, as shown in the equation below [25]. Estimating the nanofluids' specific heat is a common application of this equation. Xuan and Roetzel suggested the nanofluids' specific heat, assuming thermal equilibrium [26].

This equation is commonly used.

$$(\mathrm{C_p})_{\mathrm{nf}} = \frac{\emptyset\rho_{np}C_{P_{np}} + (1-\emptyset)\rho_{bf}C_{P_{bf}}}{\rho_{nf}} \quad (26)$$

3.3. THERMAL CONDUCTIVITY

Maxwell proposed a thermal conductivity model for solid-liquid mixes. using Effective Medium Theory [EMT] that applies to spherical particles, as seen in the equation below [27]. The thermal conductivity model applies to solid-liquid mixtures with high and low particle concentrations [24]:

$$\frac{k_{nf}}{k_{bf}} = \frac{k_p + 2k_{bf} + 2\emptyset(k_p - k_{bf})}{k_p + 2k_{bf} - \emptyset(k_p - k_{bf})} \quad (27)$$

ATU- AJIEA, Volume:1, Issue: 2, 12, 30, 2025, © 2025 AJIEA, All Rights Reserved

Al Furat Journal of Innovations in Engineering Applications (AJIEA)
ISSN - 3105-3149

3.4. DYNAMIC VISCOSITY

Although the Einstein formula is widely used to calculate dynamic viscosity, it has a problem with low volume concentration ($\phi \leq 0.02$) [28] . It is represented as follows [24]:

$$\frac{\mu_{nf}}{\mu_{bf}} = 1 + 2.5\emptyset. \qquad (28)$$

The thermophysical properties of water and nanofluids can be seen in Table 1

Table 1. Thermophysical characteristics of water and nanofluids [1].

Properties	Symbol	Unit	Pristine Water	ZnO
Density	ρ	Kg/m^3	998.2	5606
Specific Heat of nanofluid	C_p	J/Kg.K	4182	495
Thermal conductivity	k	W/m.k	0.606	60
Dynamic viscosity	μ	Pa.s(or kg/m.s)	0.00089	0.000891

3.5 Mesh Independent

Typically, unstructured matrices capable of performing complex calculations have been used; thus, selecting this unstructured tetrahedron framework was appropriate in this case. In a single step, user-ANSYS may generate solid geometry meshes as well as a whole off-site model. In the study, there were (4143760) cells randomly taken from this tetrahedron element, and element 1 mm is depicted in the Fig. 1, as follows:

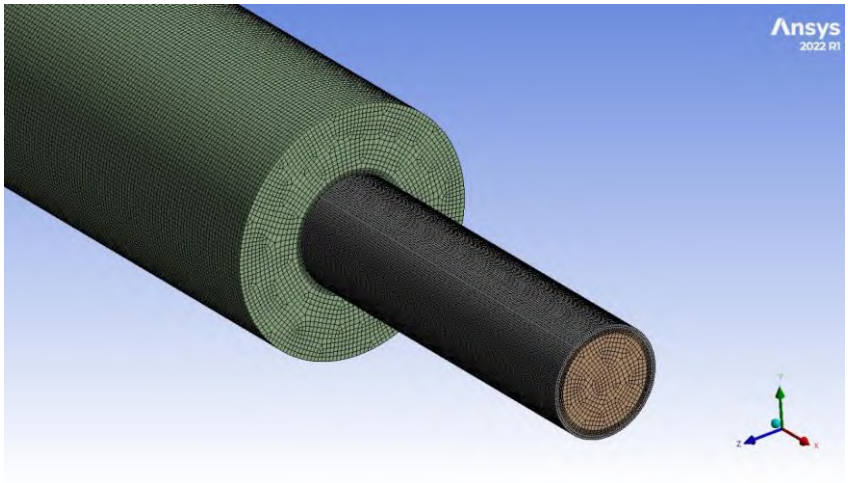

Fig. 1. Mesh generated.

A trustworthy mesh is required to solve the simulation process equation, which is determined by complicated algorithms and a high-dimensional matrix. Then, use a reliable mesh to fix the problem and restore the essential equilibrium. To mimic a diverse variety of models in the simulator, more than one mesh dependence and mesh are required

ATU- AJIEA, Volume:1, Issue: 2, 12, 30, 2025, © 2025 AJIEA, All Rights Reserved

As shown in Table (2), the element had a value of 4143760 when it reached its maximum outlet hot temperature of 317.624 k.

Table 2. Mesh independency.

Case	Element	Node	Maximum outlet hot temperature (K)	Eror %
1	1030666	1201519	320.069	0.136632
2	2129281	2357550	318.493	0.046883
3	3063790	3333790	317.623	0.002344
4	4143760	4710289	317.624	0

4. BOUNDARY CONDITION

In the numerical part, the boundary conditions are:

- Different fluid formulations (distilled water, zinc oxide)
- Inlet temperatures (45°C, and 65°C)
- Volumetric flow rates (4, and 6 liters per minute) for inner tube fluid.

Filtered water is counterflowed at a flow rate (12 liters per minute) and constant temperature (22°C) in the outer tube.

5. RESULTS AND DISCUSSION

The following is a summary of the approach applied in the double-tube heat exchanger numerical simulation using ANSYS22.0:

5.1. NUMERICAL SIMULATION OUTCOMES ANSYS

Numerical simulation results: The system temperature distribution and flow behavior were studied using the ANSYS program. The linked graphics depict pure water's temperature and pressure curves, as well as the velocity field,

The linked graphics depict "Nanoparticles at a concentration of (0.05%)" "temperature and, as well as the velocity field.

5.1.1 Temperature distribution along heat exchanger for distilled water

Figure 2 depicts the temperature contours of heat exchangers throughout the flow path for various flow rates and intake temperatures. The data show that both the rate of flow and intake temperature exhibit a direct impact on a heat exchanger's thermal performance. When the flow rate is raised to 6 LPM, the temperature distribution changes by 4 LPM. At increasing flow rates, the tube's temperature profile becomes more uniform, with relatively modest temperature changes between the input and output zone.

Lower flow rates indicate that temperature variation is steep beside the exchanger length, which means that the amount of time the fluid is forced to spend within the heat exchanger is greater; as a result, the temperature differential among the exchanger's inlet and outlet is greater. However, when the working fluid's temperature at the input rises, the influence of the temperature gradient decreases. At higher intake temperatures, the curve broadens in the high temperature area, indicating that the exchanger has a large thermal load and that heat transmission decreases as temperature rises.

ATU- AJIEA, Volume:1, Issue: 2, 12, 30, 2025, © 2025 AJIEA, All Rights Reserved

Al Furat Journal of Innovations in Engineering Applications (AJIEA)
ISSN - 3105-3149

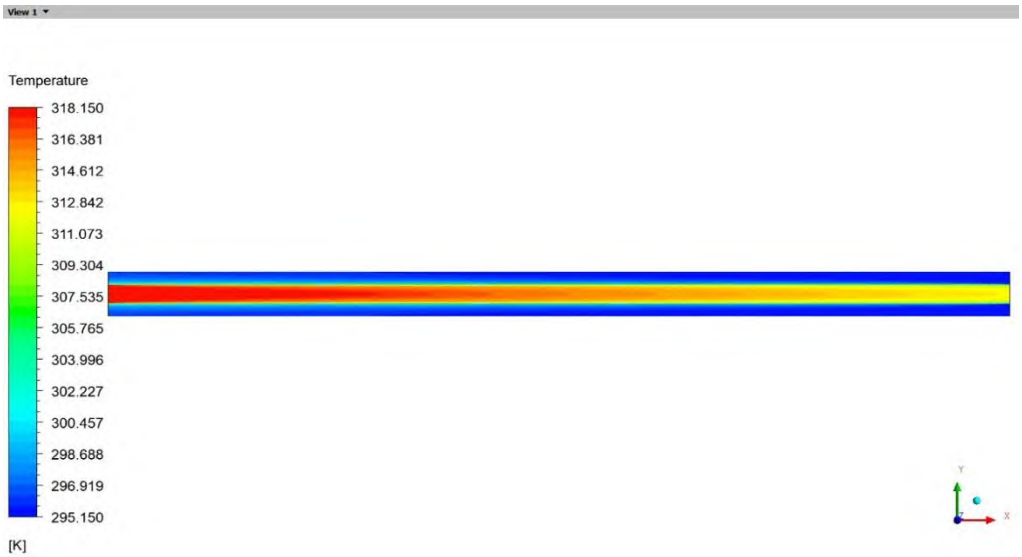

(a) 4 LPM, 45 °C

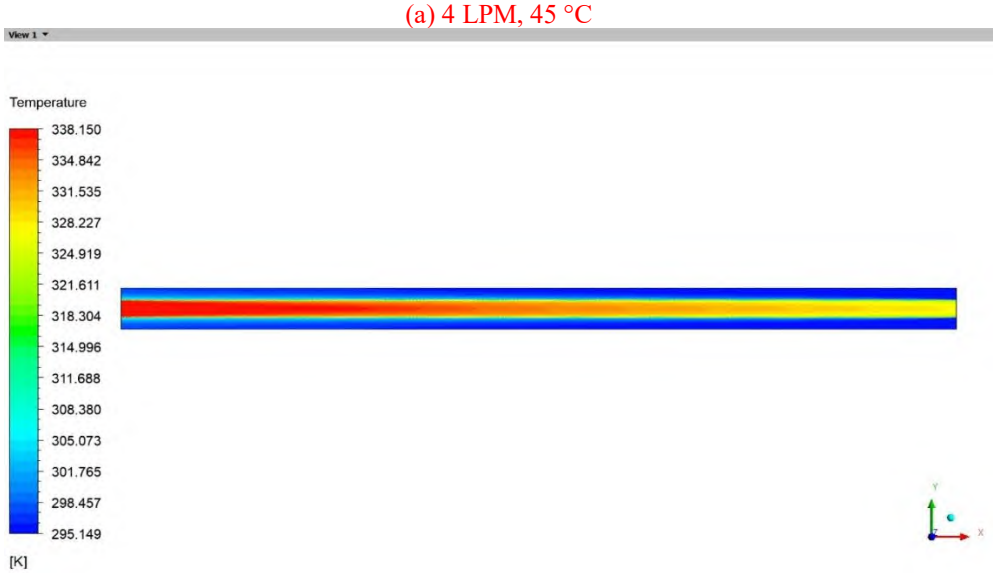

(b) 4 LPM, 65°C

ATU- AJIEA, Volume:1, Issue: 2, 12, 30, 2025, © 2025 AJIEA, All Rights Reserved

(c) 6 LPM, 45°C

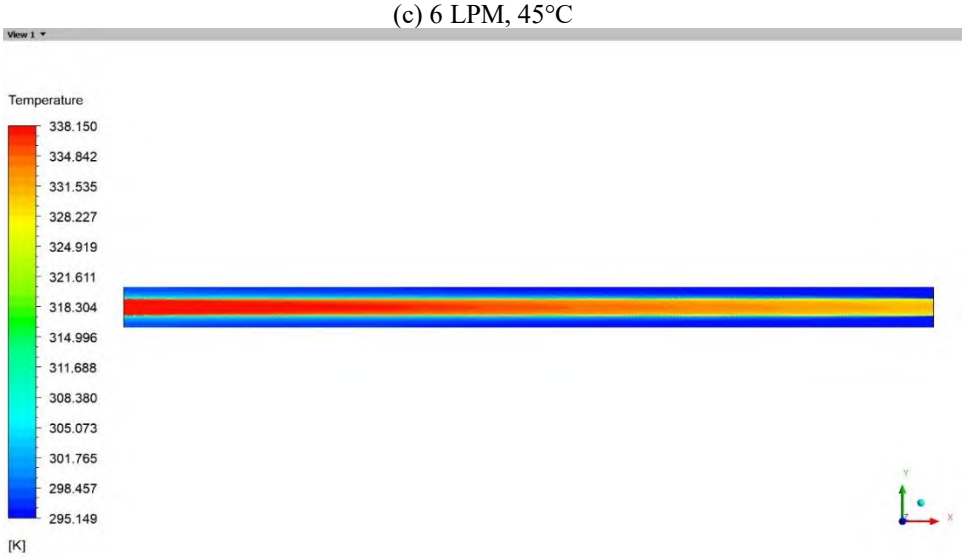

(d) 6 LPM, 65°C

Fig. 2. Temperature distribution along heat exchanger for distilled water.

According to the simulation results, the most important elements impacting the heat exchanger's thermal efficiency are flow rate with intake temperature. Higher flow rates, especially at 6 LPM, enhance heat dispersion and raise the heat transfer coefficient. Additionally, the direction of the flow has a significant impact on heat dispersion and allows for setup flexibility in response to cooling requirements. A As a result, the best operating conditions for maximum thermal efficiency are a 65°C intake temperature and a flow rate of 6 LPM.

5.1.2 Velocity distribution along heat exchanger for distilled water

The velocity distribution of distilled water passing through a heat exchanger is critical for assessing fluid dynamics and its effect on heat transfer. Fig. 3 shows rates of flow of 4LPM and 6 LPM at two definite input temperatures of 45 °C and 65 °C. The velocity distribution was as expected: at low flow rates, such as 4 LPM, the fluid flows slower near the walls and faster in the center, indicating laminar flow.

ATU- AJIEA, Volume:1, Issue: 2, 12, 30, 2025, © 2025 AJIEA, All Rights Reserved

Al Furat Journal of Innovations in Engineering Applications (AJIEA)
ISSN - 3105-3149

At high flow rates (6 LPM), the velocity of the fluid is great, resulting in a superior velocity profile throughout the exchanger. Temperature plays a larger influence, as greater temperatures result in somewhat steeper velocity profiles.

The temperature between flow rates and residence durations are critical in heat exchanger design. Higher flow rates (6 LPM) improve velocity distribution and boost heat transfer rate; nevertheless, they are not suited for applications requiring a high temperature difference between the channel's input and outflow. Lower flow rates may be more appropriate in some applications to achieve greater temperature variations.

(a) 4 LPM, 45°C

(b) 4 LPM, 65°C

ATU- AJIEA, Volume:1, Issue: 2, 12, 30, 2025, © 2025 AJIEA, All Rights Reserved

(c) 6 LPM, 45°C

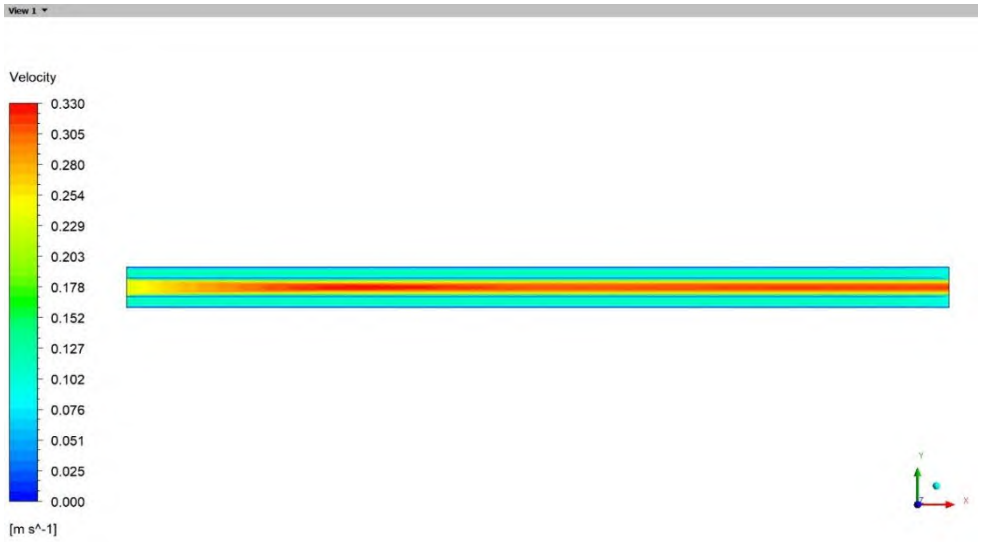

(d) 6 LPM, 65 °C

Fig. 3. Velocity distribution a long heat exchanger.

Distilled water the velocity vector profiles for distilled water in a heat exchanger at various flow rates represent both the flow's direction and intensity in the heat exchanger. This results in a less turbulent flow profile at 4 LPM, with velocity vectors dispersed uniformly and with modest magnitude. This lowered flow rate may provide greater time for heat exchange, but will establish a lower coefficient of heat transfer because of the fluid's lower velocity.

At 6 LPM, the field strength in velocity vectors is maximum, meaning that the fluid is moving very quickly in the system, resulting in quicker heat transfer rates; however, at this flow rate, the fluid time spends in the heat exchanger may be restricted. The velocity profile also introduces a unique characteristic for this flow rate: a high velocity in the core area and a reduced velocity near the wall.

ATU- AJIEA, Volume:1, Issue: 2, 12, 30, 2025, © 2025 AJIEA, All Rights Reserved

5.1.3 Pressure distribution along heat exchanger for distilled water

Figure 4 shown the pressure distribution of distilled water within the double-pipe heat exchanger was also investigated at the same flow rates (4 LPM and 6 LPM) and intake temperatures (45 and 65 °C). Unlike the velocity field, the pressure profile along the channel exhibited no fluctuation with temperature. This outcome is predicted since the fluid is basically incompressible and the enforced flow rate was maintained constant, implying that the pressure decrease is mostly determined by hydrodynamic resistance rather than thermal factors. When the input temperature was raised from 45 °C to 65 °C, the total pressure drop from inlet to exit remained practically constant for both 4 and 6 LPM. The minor drop in water viscosity at higher temperatures helps to reduce frictional losses; nevertheless, this impact was found to be minimal in the current setup, resulting in almost comparable pressure distributions. This result demonstrates that, for distilled water in this working range, flow rate is the most important element determining pressure drop, while temperature plays a minor effect. The virtually constant pressure field shows that changing the flow rate can enhance the exchanger's thermal performance without causing large pressure penalties owing to fluid heating.

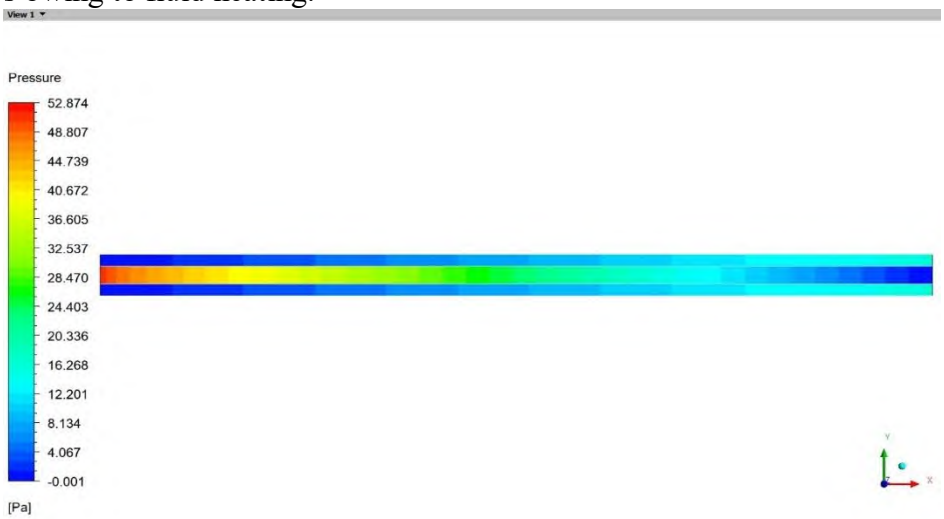

(a) 4 LPM,45 °C

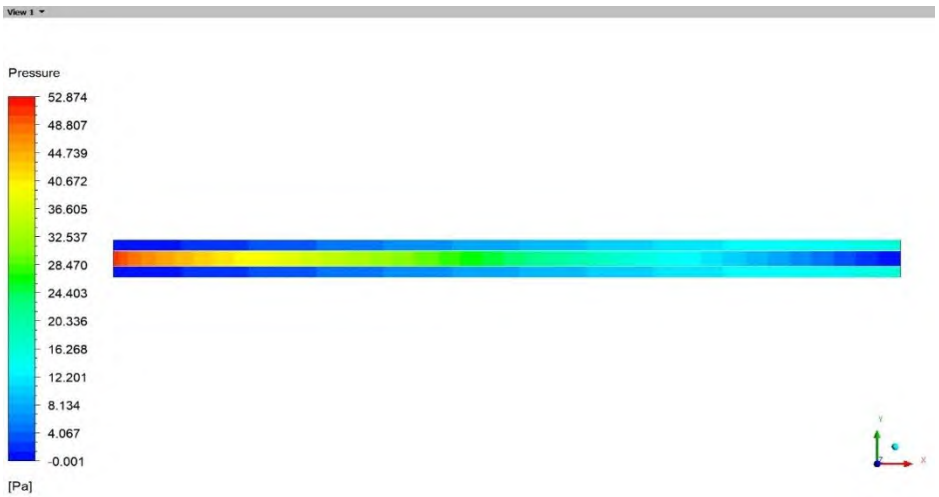

(b) 4 LPM,65 °C

ATU- AJIEA, Volume:1, Issue: 2, 12, 30, 2025, © 2025 AJIEA, All Rights Reserved

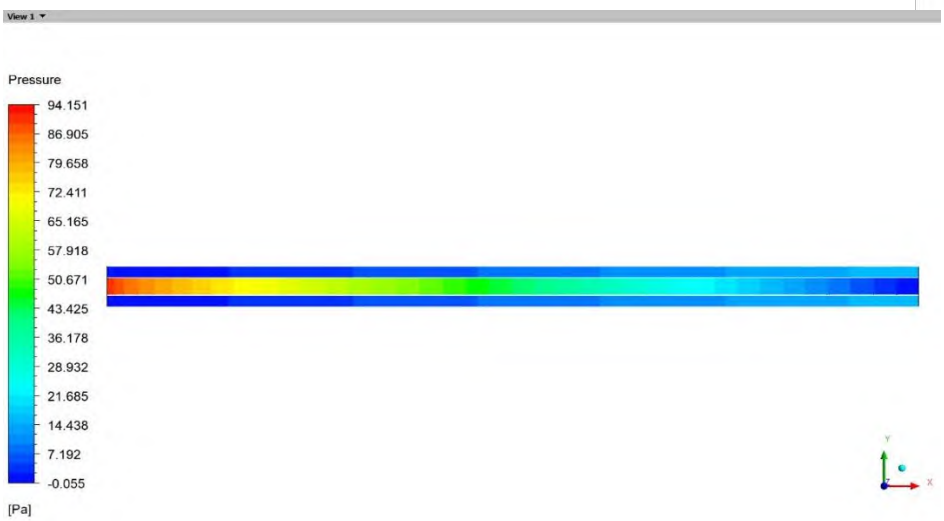

(c) 6 LPM,45 °C

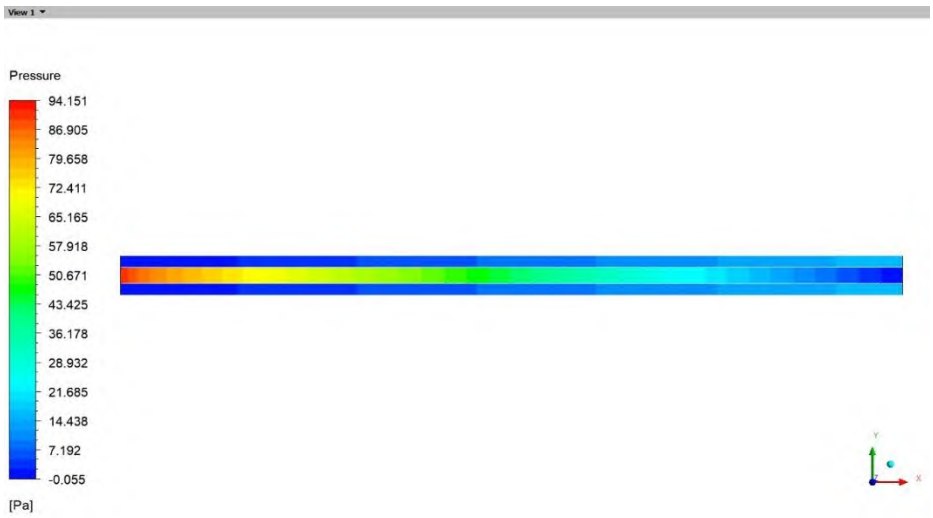

(d) 6 LPM,65 °C

Fig. 3. Pressure distribution a long heat exchanger.

The pressure drop across the heat exchanger for distilled water at different flow rates varies minimally, with variations that are nearly imperceptible. At lower flow rates, such as 4 LPM, the pressure drop is relatively modest, suggesting negligible flow resistance and consequently low pump energy usage. As the flow rate increases to 6 LPM, there is a modest increase in pressure drop owing to the greater velocity of the fluid; however, this increase is minor and has no meaningful impact on overall system performance. This small reduction in pressure drop indicates that the fluid passes effectively through the heat exchanger without incurring significant hydraulic loss.

5.1.4 Temperature distribution a long heat exchanger for ZnO+distilled water 0.05%

Figure 4 depicts the temperature fluctuation in a heat exchanger using a ZnO nanofluid that has a 0.05% concentration in volume in distilled water. The temperature distribution is displayed with regard to rates of flow of 4 LPM, and 6 LPM. Also, intake temperatures of 45°C, and 65°C. The sharp temperature gradient at lower flow rates demonstrates the increased heat transfer along the exchanger's length.

ATU- AJIEA, Volume:1, Issue: 2, 12, 30, 2025, © 2025 AJIEA, All Rights Reserved

Al Furat Journal of Innovations in Engineering Applications (AJIEA)
ISSN - 3105-3149

The fluid's temperature is more evenly distributed along its length when the flow rate is 6 LPM, since it spends less time in the heat exchanger. A decrease in the total heat transfer coefficient results from this but a greater outlet temperature, which may be beneficial in operations that demand a high outlet temperature.

The addition of ZnO nanoparticles into distilled water improves the fluid's thermal conductivity and heat transmission. Temperature distributions across several flow rates and intake temperatures show that the nanofluid's thermal efficiency is superior to that of the base fluid. Notably, at smaller rates of flow, the variance between the outflow and input temperatures becomes more dramatic, indicating more thermal energy absorption. A steeper temperature gradient at the intake is caused by this increase in thermal conductivity, enabling more efficient heat transfer during the early stages of flow development.

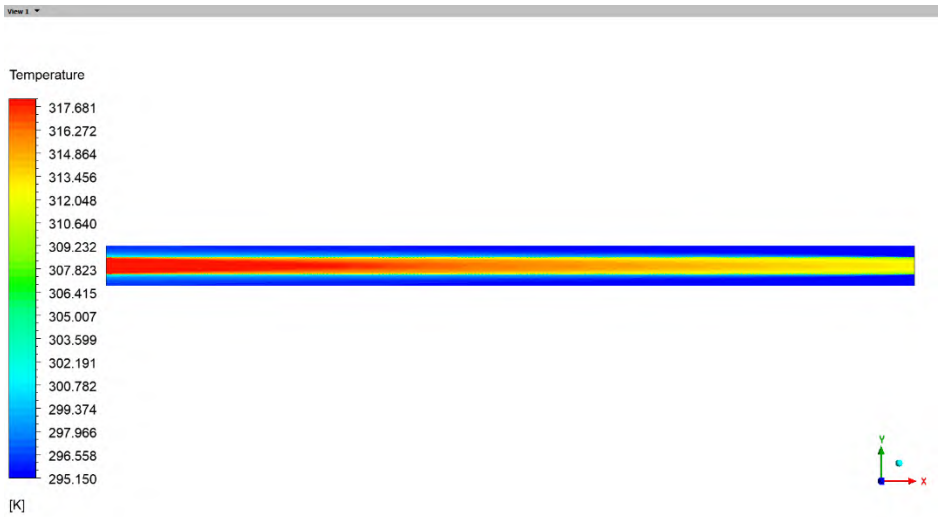

(a) 4 LPM, 45°C.

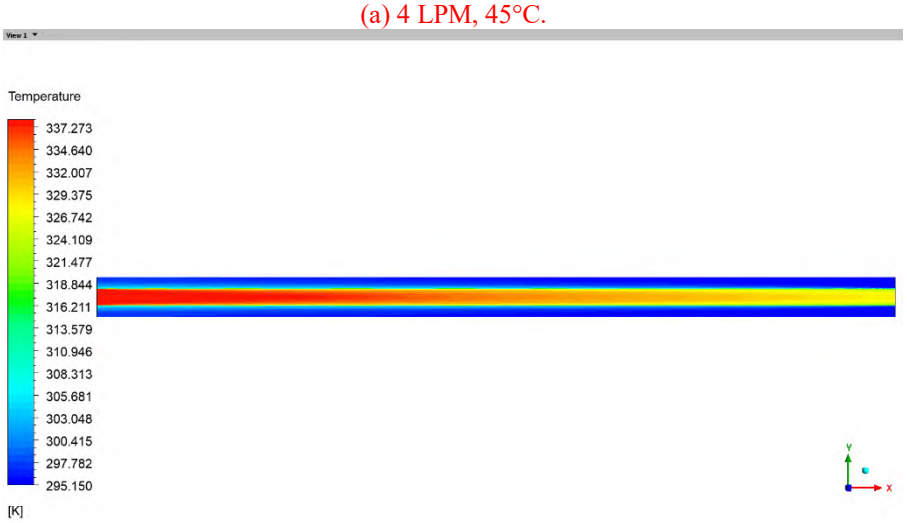

(b) 4 LPM, 65°C

ATU- AJIEA, Volume:1, Issue: 2, 12, 30, 2025, © 2025 AJIEA, All Rights Reserved

(c) 6 LPM, 45°C

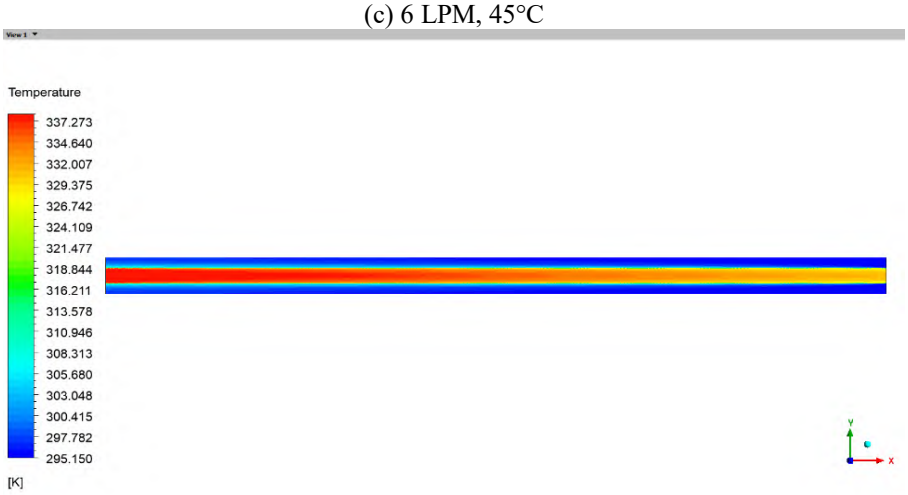

(d) 6 LPM, 65°C

Fig. 4. Temperature distribution along heat exchanger for ZnO+distilled water 0.05%.

The highest heat transfer occurs at a 4 LPM rate of flow and an input temperature of 65°C, since this condition exhibits the greatest thermal gradient due to the fluid's longer residence time in the system, allowing for more effective heat exchange. In contrast, when the same temperature is applied at a larger rate of flow of 6 LPM, heat transfer efficiency reduces because of the lower time of contact between the surface and the fluid. The total heat transmission is poorer in both flow situations at lower temperatures (45°C) because of the smaller temperature differential. When utilizing 0.05% concentration nanofluids, a higher input temperature 65°C paired with a lower flow rate 4 LPM is the best option for increasing heat transfer efficiency.

5.1.5 Velocity distribution a long heat exchanger for ZnO+distilled water 0.05%

Figure 5 shows the velocity distribution of ZnO+distilled water 0.05% by volume nanofluid in a heat exchanger, and the outcome of flow rates 4LPM and 6 LPM, and input temperatures 45 °C and 65 °C. The velocity profiles are crucial for determining the influence of the rate of flow and intake temperature on the flow phenomena within the heat exchanger.

ATU- AJIEA, Volume:1, Issue: 2, 12, 30, 2025, © 2025 AJIEA, All Rights Reserved

Al Furat Journal of Innovations in Engineering Applications (AJIEA)
ISSN - 3105-3149

The rate of flow is a crucial feature in establishing the fluid's flow features inside the heat exchanger. A greater flow rate of 6 LPM results in increased fluid velocity and velocity gradients, which improves convective mass transfer. It is also demonstrated that the effect of input temperature rises with flow rate, since higher temperatures offer more active fluid flow. High flow rates combined with high intake temperatures are indicated for increased heat transfer rate, whilst low flow rates are recommended for sustained heat transmission.

(a) 4 LPM, 45°C

(b) 4 LPM, 65°C

ATU- AJIEA, Volume:1, Issue: 2, 12, 30, 2025, © 2025 AJIEA, All Rights Reserved

(c) 6 LPM, 45°C

(d) 6 LPM, 65 °C

Fig. 5. Velocity distribution a long heat exchanger ZnO+distilled water 0.05%.

From the velocity distribution results, it is found that flow rate has a dominant effect on the fluid velocity in the pipe whereas temperature has a negligible effect. At a lower flow rate, 4 LPM (in either direction) flowing at 65°C or at 45°C the maximum velocity in the centre of the pipe is approximately 0.12 m/s This represents a much slower speed which gives more opportunity for contact with the sides of the pipe – good for heat transfer – but bad for distributing any spreadable liquids. By comparison, at 6 LPM and any temperature VI increases to approximately 0.32 m/s indicating a relatively faster and more homogenous flow. A higher flow rate (6 LPM) is also desirable from the hydraulic point of view, as it increases the velocity and enhances the dispersion along the pipe. When it comes to transmitting heat, a compromise has to be struck between flow rate and contact time. Therefore if one is trying to maximize the heat convection, 6 LPM for each of three purposes respectively proves to be the finest alternative for each working temperature even at e concentration is 0.05% nanofluid concentration.

ATU- AJIEA, Volume:1, Issue: 2, 12, 30, 2025, © 2025 AJIEA, All Rights Reserved

Al Furat Journal of Innovations in Engineering Applications (AJIEA)
ISSN - 3105-3149

5.1.6 Pressure distribution a long heat exchanger for ZnO+distilled water 0.05%

pressure drop distribution in heat exchanger for ZnO + distilled water nanofluid at 0.05% volume concentration =The pressure drop behaviour are very severe to predict the hydraulic performance and power pumping under different operational conditions. The results indicate that pressure drop remains very small for all cases considered, with changes that are practically negligible even for increased flow rate or intake temperature. Just 4 LPM, the pressure drop is little, meaning slight flow resistance and small pumping energy. At 6 LPM, higher fluid velocity causes a slight increase in pressure drop; however, this increased pressure drop is small and has no practical impact to system performance. The small variation of pressure drop confirms that, at this concentration, the addition of ZnO nanoparticles does not negatively affect the hydraulic behavior of the heat exchanger. Thus the nanofluid enhances heat transfer and reduces pumping power requirement, it provides an appreciable trade-off between enhancing heat transfer and increasing pumping power requirements.

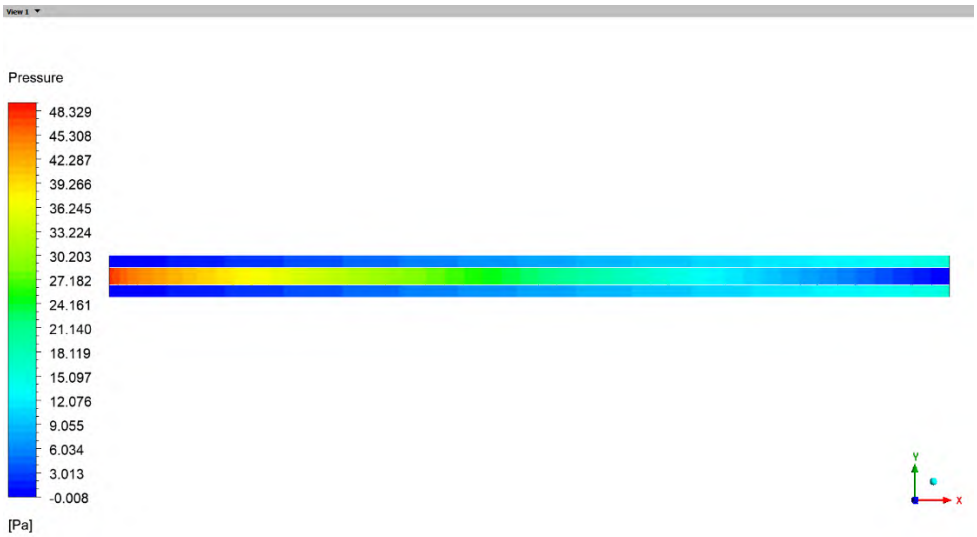

(a) 4 LPM, 45 °C.

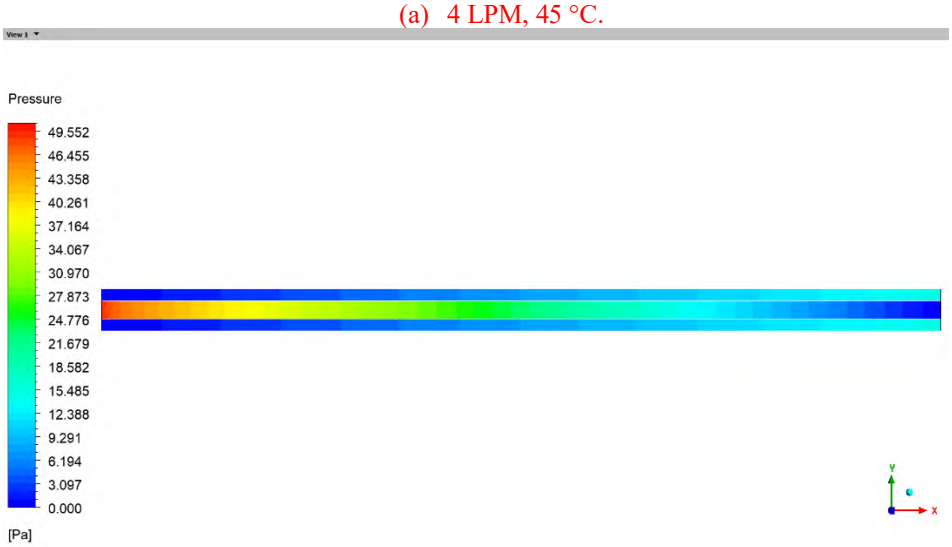

(b)4 LPM, 65 °C.

ATU- AJIEA, Volume:1, Issue: 2, 12, 30, 2025, © 2025 AJIEA, All Rights Reserved

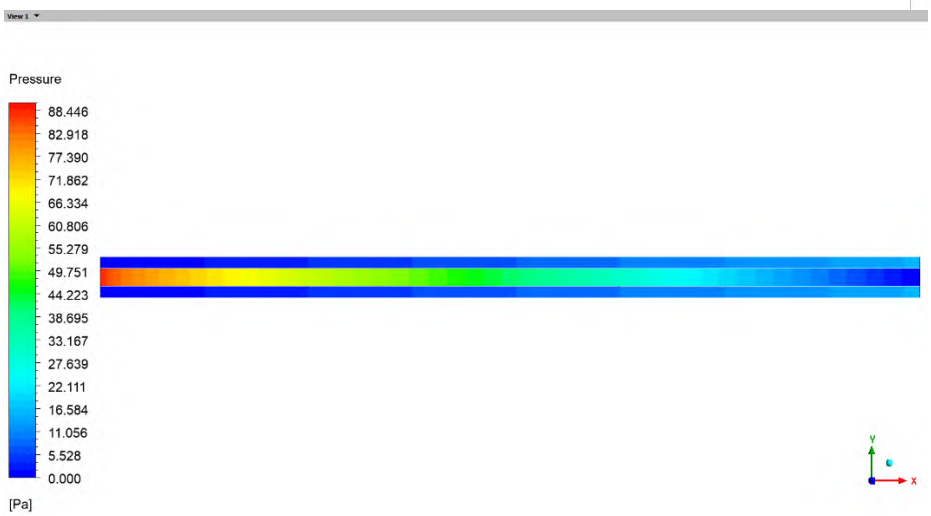

(c) 6 LPM, 45 °C

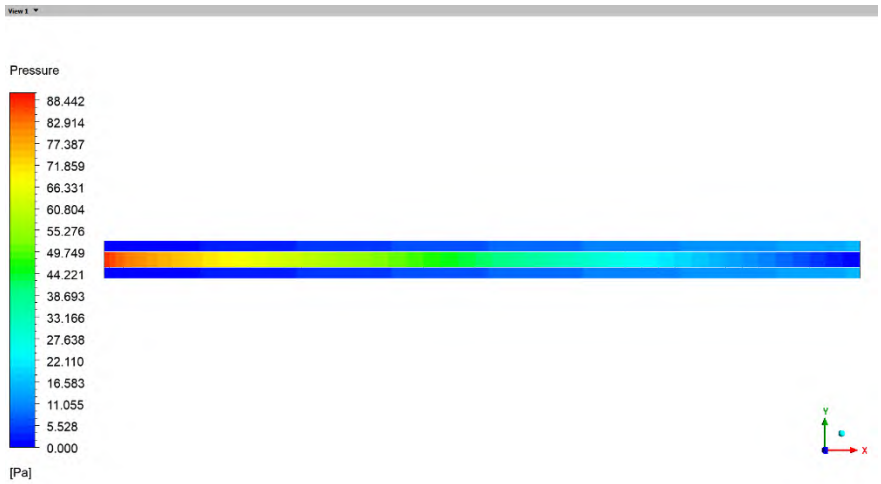

(d) 6 LPM, 65 °C

Fig. 6. pressure distribution a long heat exchanger.

Pressure drop data indicate that the flow rate significantly influences the pressure drop in the heat exchanger, and temperature has relatively little effect on the pressure drop. At lower flow rate of 4 LPM, the pressure drop is also very low for both input temperatures 45 °C and 65 °C indicating that there will be less resistance to flow as well as less energy penalty. When flow rate goes up to 6 LPM, the pressure drop increases slightly due to higher fluid velocity. Nevertheless, such is an increase, albeit a very small one and the system's hydraulic behavior would not be affected significantly. The modest effect of temperature on pressure loss indicates that changes in fluid viscosity over the range of temperatures under consideration have little effect on the flow resistance. So from a hydraulic stand point 6 LPM is optimal as velocity is increased, however, with only marginal increase in pressure loss. Such a balance favors the practical application of 0.05% nanofluids in enhancing heat exchanger performance (without substantial additional pumping costs).

5.1.7 The effectiveness vs. Temperature, the NTU vs. Temperature

The heat exchanger's performance ascended by around 30%, while the NTU, symbolizing Number of Transfer Units, improved by about 35%. This gain is attributed to the nanofluid's enhanced efficiency

ATU- AJIEA, Volume:1, Issue: 2, 12, 30, 2025, © 2025 AJIEA, All Rights Reserved

of heat flow, particularly at low concentrations, which significantly improves the system's heat transfer efficiency.

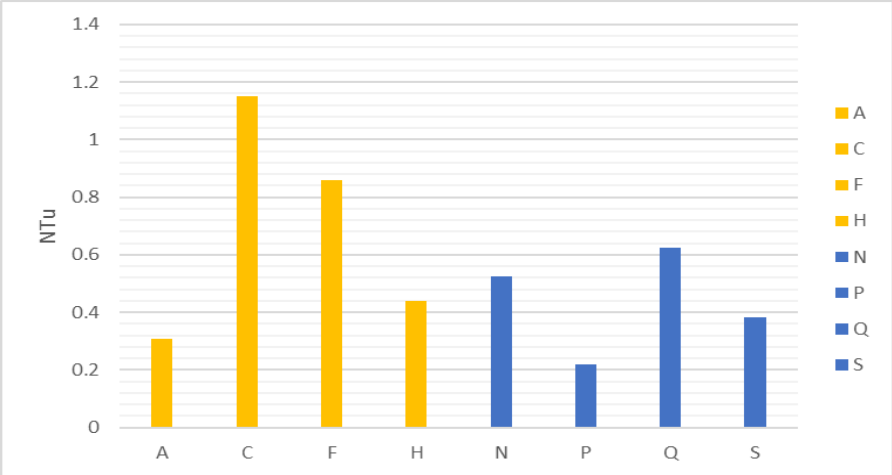

(a) the NTU and difference temperature and mass flow rate

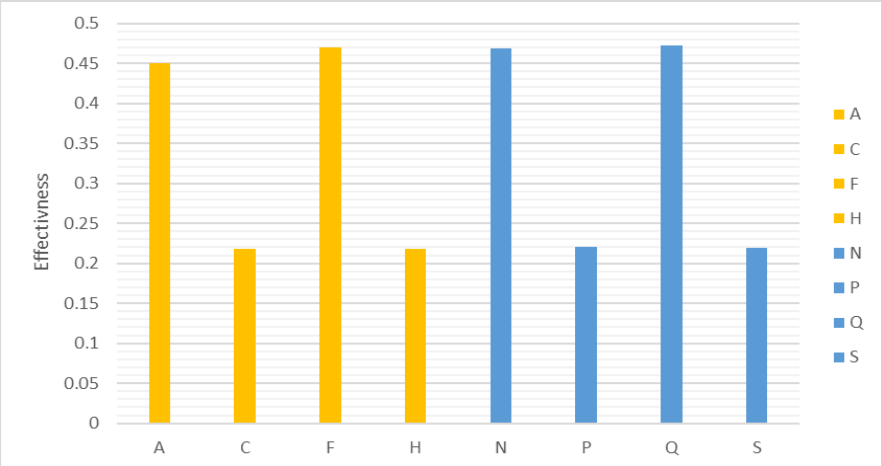

(b) The effectiveness and difference temperature and mass flow rate

Fig. 7. The results showed that, compared to pure water, using a 0.05% concentration of ZnO-based nanofluid improved the heat exchanger's efficacy.

5.1.8 The Reynolds number vs. Friction factor.

Under all measured settings, the ZnO-water nanofluid at 0.05% concentration consistently produces higher Reynolds numbers than pure distilled water, as seen in the chart. This implies improved flow dynamics and possibly increased convective heat transfer. Furthermore, the friction factor does not significantly increase, showing that the nanofluid improves thermal performance without causing large hydraulic losses. As a result, the ZnO nanofluid offers a viable solution for improving flow and heat transmission in double-pipe heat exchanger systems.

ATU- AJIEA, Volume:1, Issue: 2, 12, 30, 2025, © 2025 AJIEA, All Rights Reserved

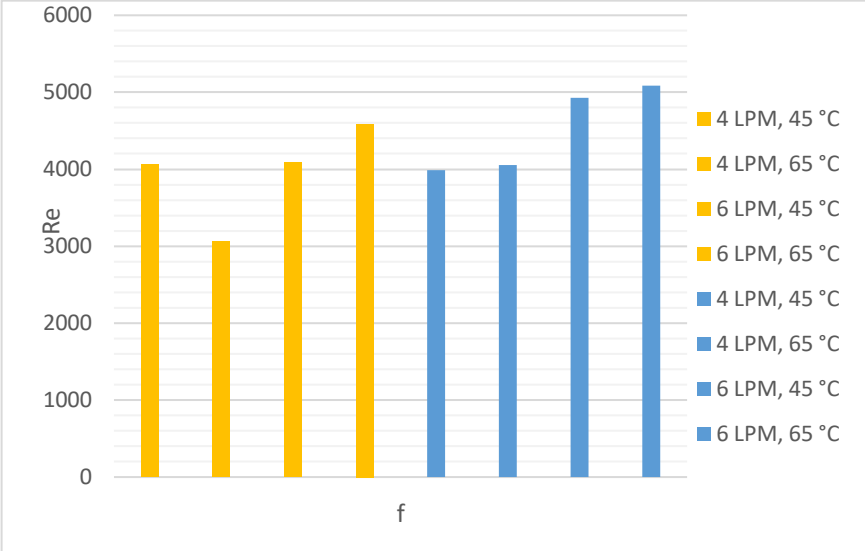

Fig. 8. The Reynolds number vs. Friction factor

5.1.9 Experimental vs. Theoretical the Reynolds number vs. Friction factor

The results show that when the Reynolds number increases, the friction factor falls in all circumstances, which is consistent with conventional correlations. However, at 65 degrees Celsius, the friction factor is constantly greater than at 45 degrees Celsius. The experimental findings demonstrate that across the analyzed Reynolds number range, the friction factor at 65 °C is roughly 15-20% larger than that at 45 °C. The difference between actual and theoretical results becomes more evident at higher temperatures because theoretical models assume constant fluid characteristics, but the thermophysical properties of nanofluids fluctuate substantially with temperature

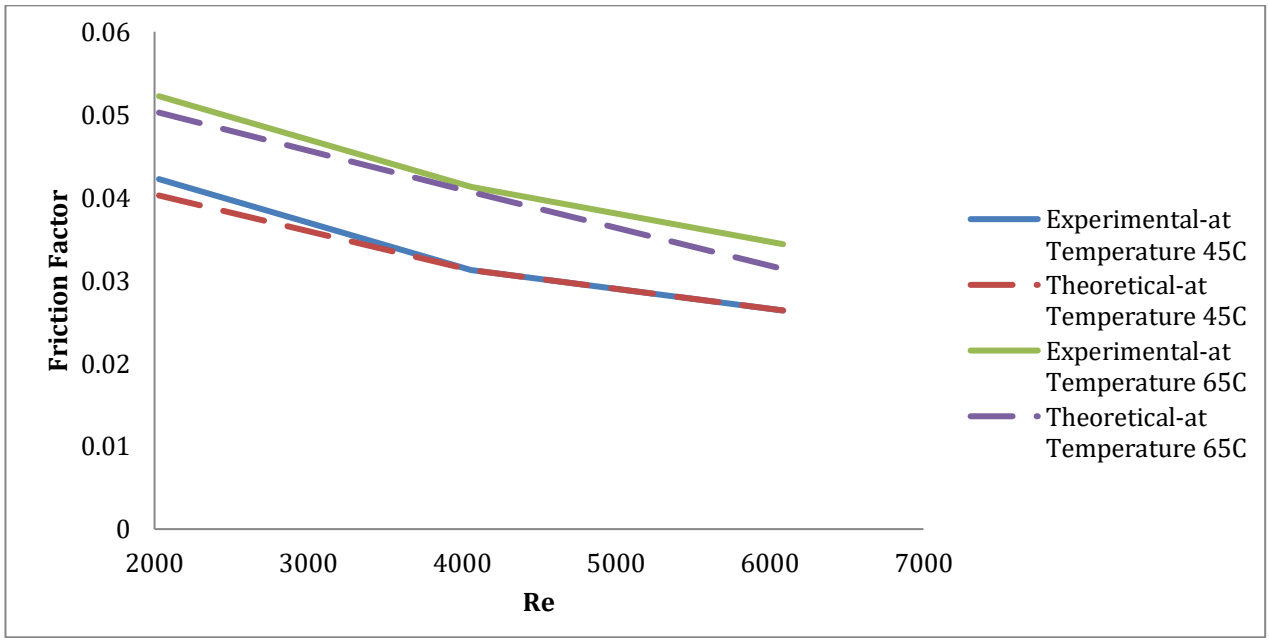

Fig. 9. Experimental vs. Theoretical the Reynolds number vs. Friction factor.

ATU- AJIEA, Volume:1, Issue: 2, 12, 30, 2025, © 2025 AJIEA, All Rights Reserved

5.1.10 Experimental vs. Theoretical the Reynolds number vs. Nusselt number

The figure shows a steady rise in the Nusselt number (Nu) with the Reynolds number (Re) at 45°C and 65°C, for both experimental and theoretical data. The concordance between experimental and theoretical data is often high, with just modest variances (about 4-8%), which are within acceptable engineering tolerances. These modest changes can be explained by practical considerations such as surface roughness, measurement inaccuracy, or minor variations in fluid characteristics. Importantly, both datasets show essentially comparable general trends and rates of Nu growth. Additionally, raising the fluid temperature from 45°C to 65°C led in a substantial increase in Nu (about 15-20%), owing to lower viscosity and enhanced thermal conductivity. The tight alignment of the two sets of findings lends evidence to the theoretical model's dependability under the test settings.

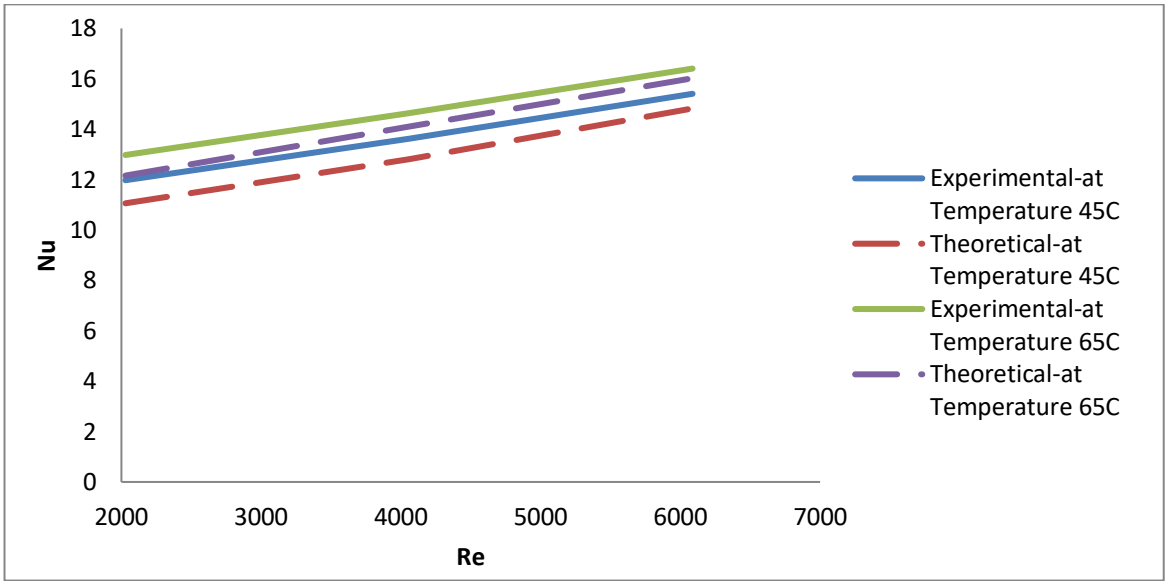

Fig. 10. Experimental vs. Theoretical the Reynolds number vs. Nusselt number.

5.1.10 Comparative assessment of thermal enhancement in ZNO nanofluids

Present study and related work. [19], a comparison of two investigations on ZnO/distilled water nanofluids at concentrations of 0.05% and 0.5% demonstrates a noticeable increase in thermal efficacy with increased nanoparticle loading. In this comparison, the 0.05% ZnO concentration relates to the current study, whereas the 0.5% concentration represents data from a prior study. At flow rates of 2, 4, and 6 L/min, the 0.5% ZnO nanofluid consistently outperformed the 0.05% equivalent in the current study, with improvements ranging from 25 to 47%. At greater particle concentrations, improved heat conductivity and micro-convection effects contribute to an increase in efficacy. Both experiments show a positive relationship between flow rate and efficacy; however, the higher concentration fluid performs much better across all test settings. These results demonstrate that raising nanoparticle concentration in nanofluids is a realistic way to enhancing heat exchanger efficiency, thereby supporting its implementation in thermal management systems.

ATU- AJIEA, Volume:1, Issue: 2, 12, 30, 2025, © 2025 AJIEA, All Rights Reserved

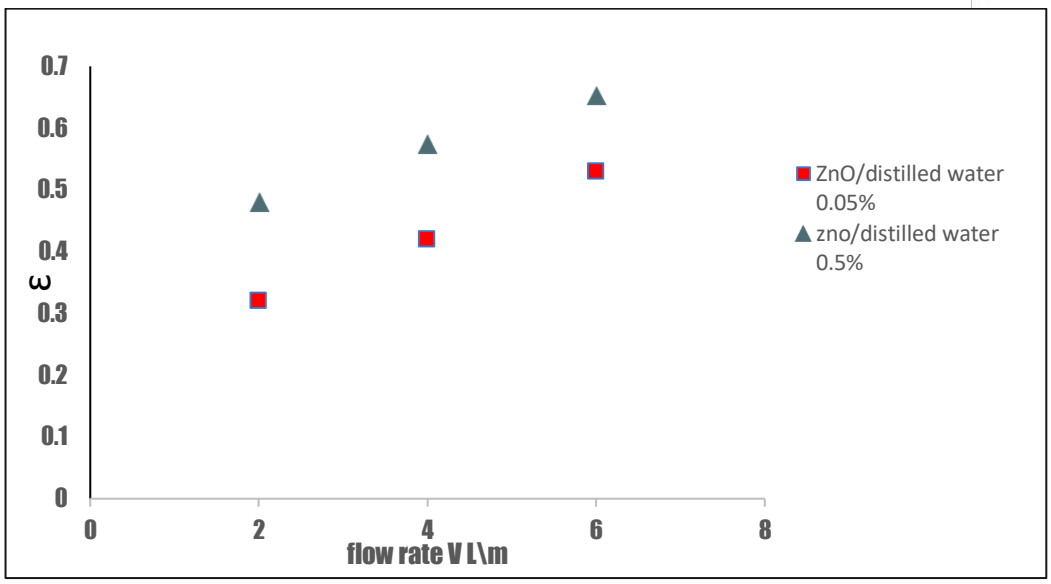

Fig. 11. Effectiveness comparison of ZnO nanofluids at different concentrations and flow rates.

6. CONCLUSION

In this work, the performance of a double-pipe heat exchanger (the inner tube is wavy) by using distilled water and 0.05% ZnO-water nanofluid was experimentally investigated. The performance enhancement of heat transfer is demonstrated approximately in the range of 25-35% at a mass flow rate of around 4 and 6 LPM when compared to pure water. In addition, its thermal efficiency enhanced by approximately 30%, due to the 7-10% enhancement of the convective heat transfer coefficient (h) and the 8-12 % improvement of the total heat transfer rate (Q). The nanofluid's thermal conductivity was also found to increase by 3-5%. These results favor ZnO-water nanofluids as perfect heat transfer promoters for industrial heat exchangers. The heat transfer improvement, without significant augmentation in the pressure drop also implies that ZnO nanofluids can be a viable alternative to using for increasing the efficiency of heat exchanger applications.

REFERENCES

[1] M. Bayareh, "Numerical simulation and analysis of heat transfer for different geometries of corrugated tubes in a double pipe heat exchanger, " Journal of thermal engineering, vol. 5, no. 4, pp. 293-301, 2019

[2] M. Omidi, M. Farhadi, and M. Jafari, "A comprehensive review on double pipe heat exchangers," Applied Thermal Engineering, vol. 110, pp. 1075–1090, 2017.

[3] B. K. Ahirwar and A. Kumar, "Experimental study of thermal performance factor for double-pipe heat exchanger using ZnO–water nanofluid," Journal of Thermal Analysis and Calorimetry, pp. 1–20, 2024.

[4] G. J. Lee, C. K. Kim, M. K. Lee, C. K. Rhee, S. Kim, and C. Kim, "Thermal conductivity enhancement of ZnO nanofluid using a one-step physical method," Thermochimica Acta, vol. 542, pp. 24–27, 2012.

ATU- AJIEA, Volume:1, Issue: 2, 12, 30, 2025, © 2025 AJIEA, All Rights Reserved

[5] K. S. Suganthi and K. S. Rajan, "Temperature induced changes in ZnO–water nanofluid: zeta potential, size distribution and viscosity profiles," International Journal of Heat and Mass Transfer, vol. 55, no. 25–26, pp. 7969–7980, 2012.

[6] R. Saleh, N. Putra, S. P. Prakoso, and W. N. Septiadi, "Experimental investigation of thermal conductivity and heat pipe thermal performance of ZnO nanofluids," International Journal of Thermal Sciences, vol. 63, pp. 125–132, 2013.

[7] S. Ferrouillat, A. Bontemps, O. Poncelet, O. Soriano, and J. A. Gruss, "Influence of nanoparticle shape factor on convective heat transfer and energetic performance of water-based SiO_2 and ZnO nanofluids," Applied Thermal Engineering, vol. 51, no. 1–2, pp. 839–851, 2013.

[8] M. J. Pastoriza-Gallego, L. Lugo, D. Cabaleiro, J. L. Legido, and M. M. Piñeiro, "Thermophysical profile of ethylene glycol-based ZnO nanofluids," The Journal of Chemical Thermodynamics, vol. 73, pp. 23–30, 2014.

[9] S. Ponmani, J. K. M. William, R. Samuel, R. Nagarajan, and J. S. Sangwai, "Formation and characterization of thermal and electrical properties of CuO and ZnO nanofluids in xanthan gum," Colloids and Surfaces A: Physicochemical and Engineering Aspects, vol. 443, pp. 37–43, 2014.

[10] R. Aghayari, H. Maddah, F. Ashori, A. Hakiminejad, and M. Aghili, "Effect of nanoparticles on heat transfer in mini double-pipe heat exchangers in turbulent flow," Heat and Mass Transfer, vol. 51, pp. 301–306, 2015.

[11] R. Islam, B. Shabani, J. Andrews, and G. Rosengarten, "Experimental investigation of using ZnO nanofluids as coolants in a PEM fuel cell," International Journal of Hydrogen Energy, vol. 42, no. 30, pp. 19272–19286, 2017.

[12] A. A. Minea and G. Lorenzini, "A numerical study on ZnO based nanofluids behavior on natural convection," International Journal of Heat and Mass Transfer, vol. 114, pp. 286–296, 2017.

[13] M. S. Alnarabiji, N. Yahya, S. Nadeem, M. Adil, M. K. Baig, O. B. Ghanem, K. Azizi, S. Ahmed, B. Maulianda, J. J. Klemeš, and K. A. Elraies, "Nanofluid enhanced oil recovery using induced ZnO nanocrystals by electromagnetic energy: Viscosity increment," Fuel, vol. 233, pp. 632–643, 2018.

[14] E. J. Onyiriuka, O. O. Ighodaro, A. O. Adelaja, D. R. E. Ewim, and S. Bhattacharyya, "A numerical investigation of the heat transfer characteristics of water-based mango bark nanofluid flowing in a double-pipe heat exchanger," Heliyon, vol. 5, no. 9, 2019.

[15] M. Armstrong, M. Sivasubramanian, and N. Selvapalam, "Experimental investigation on the heat transfer performance analysis in silver nano-coated double pipe heat exchanger using displacement reaction," Materials Today: Proceedings, vol. 45, pp. 2482–2490, 2021.

[16] A. M. Hussein and F. H. Issa, "Improve performance of double pipe heat exchanger by using ZnO/water nanofluid," Journal of Petroleum Research and Studies, vol. 13, no. 2, pp. 64–75, 2023.

[17] D. Yogaraj, S. S. K. Deepak, G. J. Rakshgan, P. Dwarakesh, R. Vishwakarma, P. K. Kujur, and Y. A. Rao, "Thermal performance analysis of a counter-flow double-pipe heat exchanger using titanium oxide and zinc oxide nanofluids," Materials Today: Proceedings, 2023.

ATU- AJIEA, Volume:1, Issue: 2, 12, 30, 2025, © 2025 AJIEA, All Rights Reserved

[18] B. K. Dandoutiya and A. Kumar, "Experimental analysis of thermal performance factor for double pipe heat exchanger with ZnO–water nanofluid," Proceedings of the Institution of Mechanical Engineers, Part E: Journal of Process Mechanical Engineering, 2023, Art. no. 09544089231175090.

[19] F. H. Issa and A. M. Hussein, "Improve performance of double pipe heat exchanger by using ZnO/water nanofluid," Journal of Petroleum Research & Studies, no. 39, pp. 64–75, Jun. 2023.

[20] Ansys Inc., "ANSYS Fluent 22.0 Theory Guide," 2022. [Online]. Available: https://dl.cfdexperts.net/cfd_resources/Ansys_Documentation/Fluent/Ansys_Fluent_Theory_Guide.pdf. [Accessed: 29-May-2025].

[21] A. İ. N. Korti, "Numerical 3-D heat flow simulations on double-pass solar collector with and without porous media," Journal of Thermal Engineering, vol. 1, no. 1, pp. 10–23, 2015.

[22] N. Sahiti, F. Durst, and A. Dewan, "Heat transfer enhancement by pin elements," International Journal of Heat and Mass Transfer, vol. 48, pp. 4738–4747, 2005.

[23] A. Fakheri, "Heat exchanger efficiency," Journal of Heat Transfer, vol. 29, no. 9, pp. 1268–1276, 2007.

[24] A. R. I. Ali and B. Salam, "A review on nanofluid: preparation, stability, thermophysical properties, heat transfer characteristics and application," SN Applied Sciences, vol. 2, no. 10, p. 1636, 2020.

[25] B. C. Pak and Y. I. Cho, "Hydrodynamic and heat transfer study of dispersed fluids with submicron metallic oxide particles," Experimental Heat Transfer an International Journal, vol. 11, no. 2, pp. 151–170, 1998.

[26] Y. Xuan and W. Roetzel, "Conceptions for heat transfer correlation of nanofluids," International Journal of Heat and Mass Transfer, vol. 43, no. 19, pp. 3701–3707, 2000.

[27] Maxwell, J. C., A Treatise on Electricity and Magnetism, Oxford, UK: Clarendon Press, 1973.

[28] M. Goodarzi, D. Toghraie, M. Reiszadeh, and M. Afrand, "Experimental evaluation of dynamic viscosity of ZnO–MWCNTs/engine oil hybrid nanolubricant based on changes in temperature and concentration," Journal of Thermal Analysis and Calorimetry, vol. 136, pp. 513–525, 2019.

ATU- AJIEA, Volume:1, Issue: 2, 12, 30, 2025, © 2025 AJIEA, All Rights Reserved